IHE 1338
pp: 1–15 (col.fig.: nil)
PROD. TYPE: COM
ED: Jolly
PAGN: Anitha - SCAN: Umesh

ARTICLE IN PRESS

PERGAMON

International Journal of Hydrogen Energy ▮▮▮ (▮▮▮▮) ▮▮▮–▮▮▮

International Journal of HYDROGEN ENERGY

www.elsevier.com/locate/ijhydene

Measurement of hydrogen balmer line broadening and thermal power balances of noble gas-hydrogen discharge plasmas

Randell L. Mills *, Andreas Voigt, Paresh Ray, Mark Nansteel, Bala Dhandapani

Black Light Power, Inc., 493 Old Trenton Road, Cranbury, NJ 08512, USA

Abstract

Line broadening of the hydrogen Balmer lines provides a sensitive measure of the number and energy of excited hydrogen atoms in a glow discharge plasma. The width of the 656.2 nm Balmer α line emitted from glow discharge plasmas having atomized hydrogen from pure hydrogen alone, hydrogen with magnesium or strontium, a mixture of 10% hydrogen and helium, argon, krypton, or xenon, and a mixture of 10% hydrogen and helium or argon with strontium was measured with a high resolution (±0.025 nm) visible spectrometer. It was found that strontium–hydrogen, helium–hydrogen, argon–hydrogen, strontium–helium–hydrogen, and strontium–argon–hydrogen plasmas showed significant broadening corresponding to an average hydrogen atom temperature of 25–45 eV; whereas, pure hydrogen, krypton–hydrogen, xenon–hydrogen, and magnesium–hydrogen showed no excessive broadening corresponding to an average hydrogen atom temperature of ≈ 3 eV. Since line broadening is a measure of the plasma temperature, and a significant difference was observed between these noble gases, the power balances of glow discharge plasmas of (1) pure krypton alone, (2) a mixture of hydrogen with argon or krypton and (3) a mixture of hydrogen and helium or argon with vaporized strontium were measured. The power emitted for power supplied to the glow discharge increased by 35–83 W depending on the presence of helium or argon and less than 1% partial pressure of strontium metal in noble gas–hydrogen mixtures. Whereas, the chemically similar noble gas krypton alone or with hydrogen had no effect on the power balance. Catalyst atoms or ions which ionize at integer multiples of the potential energy of atomic hydrogen (Sr, He^+, or Ar^+) caused an increase in power, whereas, no excess power was observed in the case of krypton which does not provide a reaction with a net enthalpy of a multiple of the potential energy of atomic hydrogen under these conditions. For a power input to the glow discharge of 110 W, the excess output power of mixtures of strontium with argon–hydrogen ($\frac{95}{5}$%), strontium with hydrogen, strontium with helium–hydrogen ($\frac{95}{5}$%), and argon–hydrogen ($\frac{95}{5}$%) was 75, 58, 50, and 28 W, respectively, based a comparison of the temperature rise of the cell with krypton–hydrogen mixture ($\frac{95}{5}$%) and krypton alone. The input power was varied to find conditions that resulted in the optimal output for the strontium–hydrogen plasma. At 136 W input, the excess power significantly increased to 184 W. These studies provide a useful comparison of catalysts for the optimization of a catalytic reaction of atomic hydrogen which represents an important new power source. © 2001 Published by Elsevier Science Ltd on behalf of the International Association for Hydrogen Energy.

1. Introduction

1.1. Background

Balmer showed in 1885 that the frequencies for some of the lines observed in the emission spectrum of atomic hydrogen could be expressed with a completely empirical relationship. This approach was later extended by Rydberg, who showed that all of the spectral lines of atomic hydrogen were given by the equation:

$$\bar{\nu} = R\left(\frac{1}{n_f^2} - \frac{1}{n_i^2}\right) \quad (1)$$

where $R = 109,677\ \mathrm{cm}^{-1}$, $n_f = 1, 2, 3, \ldots$, $n_i = 2, 3, 4, \ldots$, and $n_i > n_f$.

Niels Bohr, in 1913, developed a theory for atomic hydrogen that gave energy levels in agreement with Rydberg's equation. An identical equation, based on a totally

* Corresponding author. Tel.: +1-609-490-1090; fax: +1-609-490-1066.
E-mail address: rmills@blacklightpower.com (R.L. Mills).

0360-3199/01/$ 20.00 © 2001 Published by Elsevier Science Ltd on behalf of the International Association for Hydrogen Energy.
PII: S0360-3199(01)00172-0

different theory for the hydrogen atom, was developed by Schrödinger, and independently by Heisenberg, in 1926.

$$E_n = -\frac{e^2}{n^2 8\pi\varepsilon_o a_H} = -\frac{13.598\ \text{eV}}{n^2} \quad (2a)$$

$$n = 1, 2, 3, \ldots \quad (2b)$$

where a_H is the Bohr radius for the hydrogen atom (52.947 pm), e is the magnitude of the charge of the electron, and ε_o is the vacuum permittivity. Based on the solution of a Schrödinger-type wave equation with a nonradiative boundary condition from Maxwell's equations, Mills [1–27] predicts that atomic hydrogen may undergo a catalytic reaction with certain atomized elements or certain gaseous ions which singly or multiply ionize at integer multiples of the potential energy of atomic hydrogen, 27.2 eV. The reaction involves a nonradiative energy transfer to form a hydrogen atom that is lower in energy than unreacted atomic hydrogen that corresponds to a fractional principal quantum number where Eq. (2b) should be replaced by Eq. (2c).

$$n = 1, 2, 3, \ldots, \quad \text{and,} \quad n = \frac{1}{2}, \frac{1}{3}, \frac{1}{4}, \ldots . \quad (2c)$$

A number of independent experimental observations lead to the conclusion that atomic hydrogen can exist in fractional quantum states that are at lower energies than the traditional "ground" ($n = 1$) state.

1.2. Lower-energy hydrogen experimental data

Prior studies that support the possibility of a novel reaction of atomic hydrogen which produces a chemically generated or assisted plasma and produces novel hydride compounds include extreme ultraviolet (EUV) spectroscopy [6–11,14–18], characteristic emission from catalysis and the hydride ion products [8,9], lower-energy hydrogen emission [4,6,7], plasma formation [8–11,14,15,17,18], anomalous plasma afterglow duration [17,18], power generation [10–14,25], and analysis of chemical compounds [19–25]. Typically the emission of vacuum ultraviolet light from hydrogen gas is achieved using discharges at high voltage, synchrotron devices, high power inductively coupled plasma generators, or a plasma is created and heated to extreme temperatures by RF coupling (e.g. $> 10^6$ K) with confinement provided by a toroidal magnetic field. Observation of intense extreme ultraviolet (EUV) emission at low temperatures (e.g. $< 10^6$ K) from atomic hydrogen and certain atomized elements or certain gaseous ions [6–11,14–18] has been reported previously. The only pure elements that were observed to emit EUV were those wherein the ionization of t electrons from an atom to a continuum energy level is such that the sum of the ionization energies of the t electrons is approximately $m \cdot 27.2$ eV where t and m are each an integer. K, Cs, and Sr atoms and Rb^+ ion ionize at integer multiples of the potential energy of atomic hydrogen and caused emission. Whereas, the chemically similar atoms, Na, Mg, and Ba, do not ionize at integer multiples of the potential energy of atomic hydrogen and caused no emission. Additional prior studies that support the possibility of a novel reaction of atomic hydrogen which produces a plasma and lower-energy-hydrogen atoms, molecules, hydride ions, and novel hydride compounds include:

(1) the observation of novel EUV emission lines from microwave and glow discharges of helium with 2% hydrogen with energies of $q \cdot 13.6$ eV where $q = 1, 2, 3, 4, 6, 7, 8, 9,$ or 11 or these lines inelastically scattered by helium atoms in the excitation of He ($1s^2$) to He ($1s^1 2p^1$) that were identified as hydrogen transitions to electronic energy levels below the "ground" state corresponding to fractional quantum numbers [6],

(2) the identification of transitions of atomic hydrogen to lower energy levels corresponding to lower energy hydrogen atoms in the extreme ultraviolet emission spectrum from interstellar medium and the sun [1,4,6],

(3) the EUV spectroscopic observation of lines by the Institut für Niedertemperatur-Plasmaphysik e.V. that could be assigned to transitions of atomic hydrogen to lower energy levels corresponding to fractional principal quantum numbers and the emission from the excitation of the corresponding hydride ions [16],

(4) the recent analysis of mobility and spectroscopy data of individual electrons in liquid helium which shows direct experimental confirmation that electrons may have fractional principal quantum energy levels [5],

(5) the observation of novel EUV emission lines from microwave discharges of argon or helium with 10% hydrogen that matched those predicted for vibrational transitions of $H_2^*[n = \frac{1}{4}; n^* = 2]^+$ with energies of $v \cdot 1.185$ eV, $v = 17$–38 that terminated at the predicted dissociation limit, E_D, of $H_2[n = \frac{1}{4}]^+$, $E_D = 42.88$ eV (28.92 nm) [7],

(6) the observation of continuum state emission of Cs^{2+} and Ar^{2+} at 53.3 and 45.6 nm, respectively, with the absence of the other corresponding Rydberg series of lines from these species which confirmed the resonant nonradiative energy transfer of 27.2 eV from atomic hydrogen to the catalysts atomic Cs or Ar^+ [9],

(7) the spectroscopic observation of the predicted hydride ion $H^-(\frac{1}{2})$ of hydrogen catalysis by either Cs atom or Ar^+ catalyst at 407 nm corresponding to its predicted binding energy of 3.05 eV [9],

(8) the observation of characteristic emission from K^{3+} which confirmed the resonant nonradiative energy transfer of $3 \cdot 27.2$ eV from atomic hydrogen to atomic K [9],

(9) the spectroscopic observation of the predicted $H^-(\frac{1}{4})$ ion of hydrogen catalysis by K catalyst at 110 nm corresponding to its predicted binding energy of 11.2 eV [9],

(10) the observation by the Institut für Niedertemperatur-Plasmaphysik e.V. of an anomalous plasma and plasma afterglow duration formed with hydrogen–potassium mixtures [17],

(11) the observation of anomalous afterglow durations of plasmas formed by catalysts providing a net enthalpy of reaction within thermal energies of $m \cdot 27.28$ eV [17,18],

(12) the observation of Lyman series in the EUV that represents an energy release about 10 times that of hydrogen combustion which is greater than that of any possible known chemical reaction [6–11,14–18],

(13) the observation of line emission by the Institut für Niedertemperatur-Plasmaphysik e.V. with a 4° grazing incidence EUV spectrometer that was 100 times more energetic than the combustion of hydrogen [16],

(14) the observation of anomalous plasmas formed with Sr and Ar^+ catalysts at 1% of the theoretical or prior known voltage requirement with a light output per unit power input up to 8600 times that of the control standard light source [10,11,13,14],

(15) the observation that the optically measured output power of gas cells for power supplied to the glow discharge increased by over two orders of magnitude depending on the presence of less than 1% partial pressure of certain catalysts in hydrogen gas or argon–hydrogen gas mixtures [13],

(16) the differential scanning calorimetry (DSC) measurement of minimum heats of formation of KHI by the catalytic reaction of K with atomic hydrogen and KI that were over -2000 kJ/mole H_2 compared to the enthalpy of combustion of hydrogen of -241.8 kJ/mole H_2 [25],

(17) the isolation of novel hydrogen compounds as products of the reaction of atomic hydrogen with atoms and ions which formed an anomalous plasma as reported in the EUV studies [19–25],

(18) the identification of novel hydride compounds by (i) time of flight secondary ion mass spectroscopy which showed a dominant hydride ion in the negative ion spectrum, (ii) X- ray photoelectron spectroscopy which showed novel hydride peaks and significant shifts of the core levels of the primary elements bound to the novel hydride ions, (iii) ^1H nuclear magnetic resonance spectroscopy (NMR) which showed extraordinary upfield chemical shifts compared to the NMR of the corresponding ordinary hydrides, and (iv) thermal decomposition with analysis by gas chromatography, and mass spectroscopy which identified the compounds as hydrides [19–25],

(19) the NMR identification of novel hydride compounds MH^*X wherein M is the alkali or alkaline earth metal, X, is a halide, and H^* comprises a novel high binding energy hydride ion identified by a large distinct upfield resonance [19–24],

(20) the replication of the NMR results of the identification of novel hydride compounds by large distinct upfield resonances at Spectral Data Services, University of Massachusetts Amherst, University of Delaware, Grace Davison, and National Research Council of Canada [19], and

(21) the NMR identification of novel hydride compounds MH^* and MH_2^* wherein M is the alkali or alkaline earth metal and H^* comprises a novel high binding energy hydride ion identified by a large distinct upfield resonance that proves the hydride ion is different from the hydride ion of the corresponding known compound of the same composition [19].

1.3. Mechanism of the formation of lower-energy atomic hydrogen

The mechanism of the EUV emission, the formation of novel hydrides, and the observation of certain EUV lines from interstellar medium and the sun cannot be explained by the conventional energy levels of hydrogen, but it is predicted by a solution of the Schrödinger equation with a nonradiative boundary constraint put forward by Mills [1]. Mills predicts that certain atoms or ions serve as catalysts to release energy from hydrogen to produce an increased binding energy hydrogen atom called a *hydrino atom* having a binding energy given by Eq. (2a) where

$$n = \frac{1}{2}, \frac{1}{3}, \frac{1}{4}, \ldots, \frac{1}{p} \quad (3)$$

and p is an integer greater than 1, designated as $H[a_H/p]$ where a_H is the radius of the hydrogen atom. Hydrinos are predicted to form by reacting an ordinary hydrogen atom with a catalyst having a net enthalpy of reaction of about

$$m \cdot 27.2 \text{ eV} \quad (4)$$

where m is an integer. This catalysis releases energy from the hydrogen atom with a commensurate decrease in size of the hydrogen atom, $r_n = na_H$. For example, the catalysis of $H(n = 1)$ to $H(n = \frac{1}{2})$ releases 40.8 eV, and the hydrogen radius decreases from a_H to $\frac{1}{2}a_H$.

The excited energy states of atomic hydrogen are also given by Eq. (2a) except with Eq. (2b). The $n = 1$ state is the "ground" state for "pure" photon transitions (the $n = 1$ state can absorb a photon and go to an excited electronic state, but it cannot release a photon and go to a lower-energy electronic state). However, an electron transition from the ground state to a lower-energy state is possible by a nonradiative energy transfer such as multipole coupling or a resonant collision mechanism. These lower-energy states have fractional quantum numbers, $n = (1/\text{integer})$.

Processes that occur without photons and that require collisions are common. For example, the exothermic chemical reaction of H+H to form H_2 does not occur with the emission of a photon. Rather, the reaction requires a collision with a third body, M, to remove the bond energy-H + H + M → $H_2 + H^*$ [28]. The third body distributes the energy from the exothermic reaction, and the end result is the H_2 molecule and an increase in the temperature of the system. Some commercial phosphors are based on nonradiative energy transfer involving multipole coupling. For example, the strong absorption strength of Sb^{3+} ions along with the efficient nonradiative transfer of excitation from Sb^{3+} to Mn^{2+} are responsible for the strong manganese luminescence from phosphors containing these ions [29]. Similarly, the $n = 1$ state of hydrogen and the $n = (1/\text{integer})$ states of hydrogen are nonradiative, but a transition between two nonradiative states is possible via a nonradiative energy transfer, say $n = 1$ to $n = \frac{1}{2}$. In these cases, during the transition the electron couples to another electron transition, electron transfer

reaction, or inelastic scattering reaction which can absorb the exact amount of energy that must be removed from the hydrogen atom to cause the transition. Thus, a catalyst provides a net positive enthalpy of reaction of $m \cdot 27.2$ eV (i.e. it absorbs $m \cdot 27.2$ eV where m is an integer). Certain atoms or ions serve as catalysts which resonantly accept energy from hydrogen atoms and release the energy to the surroundings to effect electronic transitions to fractional quantum energy levels.

The catalysis of hydrogen involves the nonradiative transfer of energy from atomic hydrogen to a catalyst which may then release the transferred energy by radiative and nonradiative mechanisms. As a consequence of the nonradiative energy transfer, the hydrogen atom becomes unstable and emits further energy until it achieves a lower-energy nonradiative state having a principal energy level given by Eqs. (2a) and (3).

1.4. Catalysts

1.4.1. Argon ion

Argon ions can provide a net enthalpy of a multiple of that of the potential energy of the hydrogen atom. The second ionization energy of argon is 27.63 eV. The reaction Ar^+ to Ar^{2+} has a net enthalpy of reaction of 27.63 eV, which is equivalent to $m = 1$ in Eq. (4).

$$27.63 \text{ eV} + Ar^+ + H\left[\frac{a_H}{p}\right] \rightarrow Ar^{2+} + e^- + H\left[\frac{a_H}{(p+1)}\right] + [(p+1)^2 - p^2]X13.6 \text{ eV}, \quad (5)$$

$$Ar^{2+} + e^- \rightarrow Ar^+ + 27.63 \text{ eV}, \quad (6)$$

and, the overall reaction is

$$H\left[\frac{a_H}{p}\right] \rightarrow H\left[\frac{a_H}{(p+1)}\right] + [(p+1)^2 - p^2]X13.6 \text{ eV}. \quad (7)$$

The energy given off during catalysis is much greater than the energy lost to the catalyst. The energy released is large compared to conventional chemical reactions. For example, when hydrogen and oxygen gases undergo combustion to form water

$$H_2(g) + \tfrac{1}{2}O_2(g) \rightarrow H_2O(l) \quad (8)$$

the known enthalpy of formation of water is $\Delta H_f = -286$ kJ/mole or 1.48 eV per hydrogen atom. By contrast, each ($n = 1$) ordinary hydrogen atom undergoing catalysis releases a net of 40.8 eV. Moreover, further catalytic transitions may occur: $n = \frac{1}{2} \rightarrow \frac{1}{3}$, $\frac{1}{3} \rightarrow \frac{1}{4}$, $\frac{1}{4} \rightarrow \frac{1}{5}$, and so on. Once catalysis begins, hydrinos autocatalyze further in a process called *disproportionation*. This mechanism is similar to that of an inorganic ion catalysis. But, hydrino catalysis should have a higher reaction rate than that of the inorganic ion catalyst due to the better match of the enthalpy to $m \cdot 27.2$ eV.

1.4.2. Helium ion

Helium ion (He^+) is also such a catalyst because the second ionization energy of helium is 54.417 eV, which is equivalent to $m = 2$ in Eq. (4). In this case, the catalysis reaction is

$$54.417 \text{ eV} + He^+ + H[a_H] \rightarrow He^{2+} + e^- + H\left[\frac{a_H}{3}\right] + 108.8 \text{ eV}, \quad (9)$$

$$He^{2+} + e^- \rightarrow He^+ + 54.417 \text{ eV}, \quad (10)$$

and, the overall reaction is

$$H[a_H] \rightarrow H\left[\frac{a_H}{3}\right] + 54.4 \text{ eV} + 54.4 \text{ eV}. \quad (11)$$

1.4.3. Atomic strontium

Strontium atoms can provide a net enthalpy of a multiple of that of the potential energy of the hydrogen atom. The first through the fifth ionization energies of strontium are 5.69484, 11.03013, 42.89, 57, and 71.6 eV, respectively [30]. The ionization reaction of Sr to Sr^{5+}, ($t = 5$), then, has a net enthalpy of reaction of 188.2 eV, which is equivalent to $m = 7$ in Eq. (4).

$$188.2 \text{ eV} + Sr(m) + H\left[\frac{a_H}{p}\right] \rightarrow Sr^{5+} + 5e^- + H\left[\frac{a_H}{(p+7)}\right] + [(p+7)^2 - p^2]X13.6 \text{ eV}, \quad (12)$$

$$Sr^{5+} + 5e^- \rightarrow Sr(m) + 188.2 \text{ eV}, \quad (13)$$

and, the overall reaction is

$$H\left[\frac{a_H}{p}\right] \rightarrow H\left[\frac{a_H}{(p+7)}\right] + [(p+7)^2 - p^2]X13.6 \text{ eV}. \quad (14)$$

For strontium, the ionization data is only given to two significant figures [31]; whereas, at least three are needed to calculate the enthalpy of reaction to determine whether it is a catalyst. Since the available data indicates that strontium may provide an enthalpy of reaction that is within about 1% of $m \cdot 27.2$ eV, it was anticipated and confirmed to be catalyst [10,11,13–15].

Xenon is unlikely a catalyst since the candidate reaction involving the ionization of Xe^+ to Xe^{3+} is 53.3328 eV rather than 54.4 eV. Krypton may be a catalyst, but is less likely since the candidate reaction Kr to Kr^{6+} is 271 eV rather than 272 eV; however, the available ionization data [30] is not known to sufficient accuracy. A neon ion and a proton can also provide a net enthalpy of a multiple of that of the potential energy of the hydrogen atom; thus, neon may be a catalyst in a very intense neon–hydrogen plasma. The

second ionization energy of neon is 40.96 eV, and H^+ releases 13.6 eV when it is reduced to H. The combination of reactions of Ne^+ to Ne^{2+} and H^+ to H, then, has a net enthalpy of reaction of 27.36 eV, which is equivalent to $m = 1$ in Eq. (4). Neon is not covered in this report, but is the subject of a report in progress.

The published ionization potentials are a good guide to predict catalysts and have been remarkably successful [8–11,14,15,17,18], but in some cases, the ionization data is incomplete [30]. Experimental condition-dependent catalytic rates are also a consideration. The absolute means to evaluate catalysts are experimental tests. Two methods are the formation of a plasma by incandescent heating the source of catalyst in the presence of atomic hydrogen [15] and line broadening which was measured in the present work.

1.5. Initial optical and thermal power balance measurements

Glow discharge devices have been developed over decades as light sources, ionization sources for mass spectroscopy, excitation sources for optical spectroscopy, and sources of ions for surface etching and chemistry [31–33]. A Grimm-type glow discharge is a well established excitation source for the analysis of conducting solid samples by optical emission spectroscopy [34–36]. Despite extensive performance characterizations, data was lacking on the plasma parameters of these devices. Kuraica and Konjevic [37] and Videnocic et al. [38] have characterized these plasmas by determining the excited hydrogen atom concentrations and energies from measurements of the line broadening of the 656.2 nm Balmer α line.

A new previously reported plasma source [8–11,14,15,17,18] has been developed that operates by incandescently heating a hydrogen dissociator and a catalyst to provide atomic hydrogen and gaseous catalyst, respectively, such that the catalyst reacts with the atomic hydrogen to produce a plasma. It was extraordinary, that intense EUV emission was observed by Mills et al. [8–11,14,15,17,18] at low temperatures (e.g. $\approx 10^5$ K) from atomic hydrogen and certain atomized elements or certain gaseous ions which singly or multiply ionize at integer multiples of the potential energy of atomic hydrogen, 27.2 eV that comprise catalysts.

Furthermore, Mills et al. [10,11,14] have reported that strontium atoms each ionize at an integer multiple of the potential energy of atomic hydrogen and caused intense EUV emission. The enthalpy of ionization of Sr to Sr^{5+} has a net enthalpy of reaction of 188.2 eV, which is equivalent to $m = 7$. The emission intensity of the plasma generated by atomic strontium increased significantly with the introduction of argon gas only when Ar^+ emission was observed. Whereas, no emission was observed when chemically similar atoms that do not ionize at integer multiples of the potential energy of atomic hydrogen (sodium, magnesium, or barium) replaced strontium with hydrogen, hydrogen–argon mixtures, or strontium alone.

The power balance of a gas cell having vaporized strontium and atomized hydrogen from pure hydrogen or argon–hydrogen mixture ($\frac{77}{23}$%) was measured by integrating the total light output corrected for spectrometer system response and energy over the visible range [11]. Hydrogen control cell experiments were identical except that sodium, magnesium, or barium replaced strontium. In the case of hydrogen–sodium, hydrogen–magnesium, and hydrogen–barium mixtures, 4000, 7000, and 6500 times the power of the hydrogen–strontium mixture was required, respectively, in order to achieve that same optically measured light output power. With the addition of argon to the hydrogen–strontium plasma, the power required to achieve that same optically measured light output power was reduced by a factor of about two. The power required to maintain a plasma of equivalent optical brightness with strontium atoms present was 8600 and 6300 times less than that required for argon–hydrogen and argon control, respectively. A plasma formed at a cell voltage of about 250 V for hydrogen alone and sodium–hydrogen mixtures, 140 –150 V for hydrogen–magnesium and hydrogen–barium mixtures, 224 V for an argon–hydrogen mixture, and 190 V for argon alone; whereas, a plasma formed for hydrogen–strontium mixtures and argon–hydrogen–strontium mixtures at extremely low voltages of about 2 and 6.6 V, respectively.

The power balances of gas plasmas having atomized hydrogen from pure hydrogen alone, an argon–hydrogen mixture alone, or pure hydrogen or an argon–hydrogen mixture with vaporized potassium, rubidium, cesium, strontium, sodium, or magnesium were previously reported [13]. The power was measured by integrating the total light output corrected for spectrometer system response and energy over the visible range as the input power was varied. The light emitted per unit power supplied to the glow discharge increased by over two orders of magnitude depending on the presence of less than 1% partial pressure of certain of the alkali or alkaline earth metals in hydrogen gas or argon–hydrogen gas mixtures. Whereas, other chemically similar metals had no effect on the plasma. The metal vapor enhancement of the emission was dramatically greater with an argon–hydrogen mixture versus pure hydrogen, and a 97% argon and 3% hydrogen mixture had greater emission than either gas alone. Only those atoms or ions which ionize at integer multiples of the potential energy of atomic hydrogen, K, Cs, Rb^+, Sr, and Ar^+ caused an anomalous increase in emission; whereas, no anomalous behavior was observed in the case of Mg and Na which do not provide a reaction with a net enthalpy of a multiple of the potential energy of atomic hydrogen. The light intensity versus power input of a mixture of these metals with hydrogen, argon, or argon–hydrogen gas was the same as that of the corresponding gas alone. At an input power to the glow discharge of 10 W, the optically measured light output power of a mix-

ture of strontium, cesium, potassium, or rubidium with 97% argon and 3% hydrogen was 750, 70, 16, and 13 $\mu W/cm^2$, respectively [13]. Whereas, the optically measured light output power of the argon–hydrogen mixture ($\frac{97}{3}$%) alone or with sodium or magnesium was about 11 $\mu W/cm^2$, and the result for hydrogen or argon alone was 1.5 $\mu W/cm^2$. An excess thermal balance of 42 W was measured for the 97% argon and 3% hydrogen mixture versus argon plasma alone.

To further study the mechanism of the excess optical power balances, the width of the 656.2 nm Balmer α line emitted from glow discharge plasmas having atomized hydrogen from pure hydrogen alone, hydrogen with magnesium or strontium, and noble gas–hydrogen mixtures alone or with strontium was measured with a high resolution (±0.025 nm) visible spectrometer. Since line broadening is a measure of the plasma temperature, and a significant difference was observed between these noble gases and due to the presence of strontium, the power balances of glow discharge plasmas were measured by heat loss calorimetry (determining the power balance from the temperature at steady state relative to that of a control power source) as the input power was varied.

2. Experimental

2.1. High resolution visible spectroscopy

The width of the 656.2 nm Balmer α line emitted from glow discharge plasmas having atomized hydrogen from pure hydrogen alone, hydrogen with magnesium or strontium, a mixture of 10% hydrogen and helium, argon, krypton, or xenon, and a mixture of 10% hydrogen and helium or argon with strontium was measured with a high resolution visible spectrometer at Jobin Yvon Horiba, Inc, Edison, NJ. The plasmas were carried out in the cylindrical stainless steel gas cell shown in Fig. 1 and described in Section 2.2. The spectrometer was a TRIAX 550 Spectrometer with a standard PMT detector that had a resolution of ±0.025 nm over the spectral range 190–860 nm. A UV-grade sapphire window described in Section 2.2 provided a visible light path from inside the cell. The plasma emission from the glow discharges was fiber-optically coupled to the spectrometer through a 220F matching fiber adapter. The entrance and exit slits were set to 20 μm. The spectrometer was scanned between 656–657 nm using a 0.01 nm step size. The signal was recorded by a PMT (Hamamatsu R928) with a stand

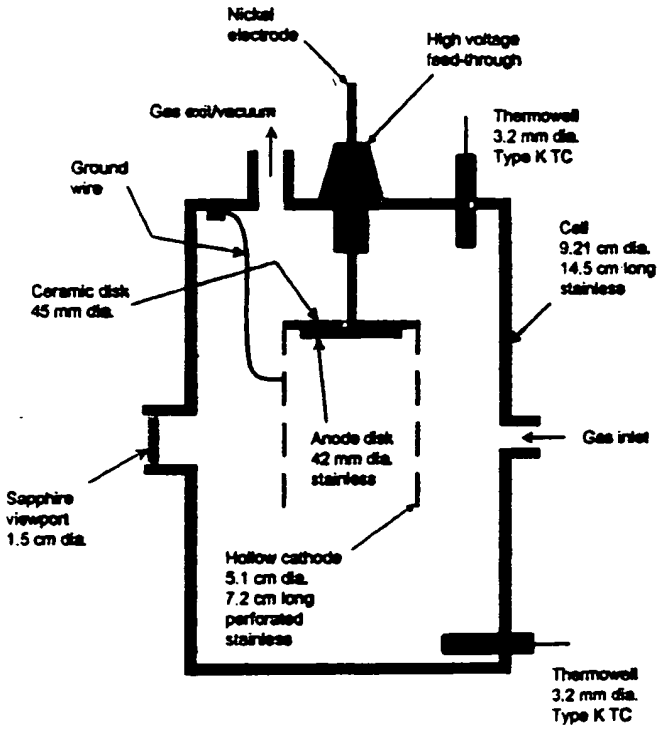

Fig. 1. Cylindrical stainless steel glow discharge cell for 656.2 nm Balmer α line width and power balance studies.

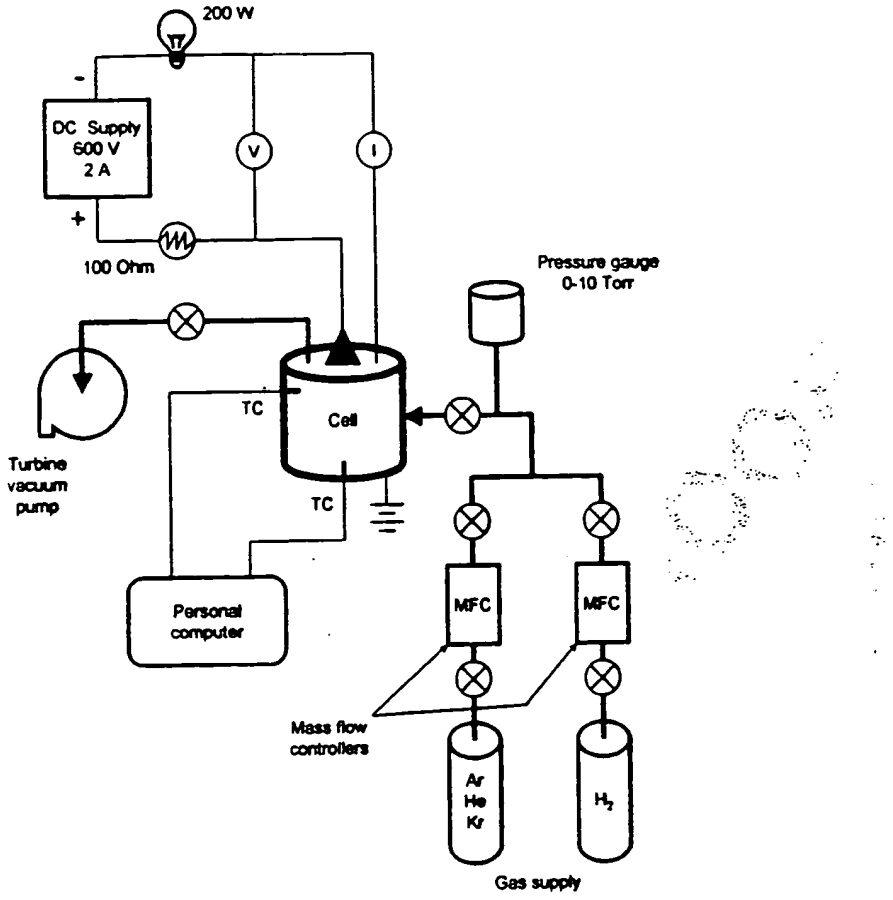

Fig. 2. The experimental setup for generating a glow discharge plasma and for measuring the power balance.

alone high voltage power supply (950 V) and an acquisition controller (SpectrAcq 2). The data was obtained in a single accumulation with a 1 s integration time.

2.2. Power cell apparatus and procedure

Power balances were measured on plasmas with (1) krypton alone, (2) krypton–hydrogen mixture ($\frac{95}{5}$%), (3) a mixture of hydrogen and vaporized strontium, (4) argon–hydrogen mixture ($\frac{95}{5}$%), and (5) a helium–hydrogen mixture ($\frac{95}{5}$%) or an argon–hydrogen mixture ($\frac{95}{5}$%) with vaporized strontium. The plasmas were maintained in the cylindrical stainless steel gas cell shown in Fig. 1, and the power was measured by heat loss calorimetry as the input power was varied. The experimental setup for generating a glow discharge plasma and for measuring the power balance is shown in Fig. 2. All experiments were performed in a clean room having a controlled ambient temperature of ±0.1°C.

The 304-stainless steel cylindrical cell was 9.21 cm in diameter and 14.5 cm in height. The base of the cell contained a welded-in stainless steel thermocouple well (1 cm OD) which housed a thermocouple in the cell interior approximately 2 cm from the discharge and 2 cm from the cell axis. The top end of the cell was welded to a high vacuum 11.75 cm diameter conflat flange. A silver plated copper gasket was placed between a mating flange and the cell flange. The two flanges were clamped together with 10 circumferential bolts. The mating flange contained four penetrations comprising (1) a stainless steel thermocouple well (1 cm OD) which also housed a thermocouple in the cell interior approximately 2 cm from the discharge and 2 cm from the cell axis, (2) a centered high voltage feedthrough which transmitted the power, supplied through a power connector, to a hollow cathode inside the cell, and (3) two stainless steel tubes (0.95 cm diameter and 100 cm in length) with one welded flush with the bottom surface of the top flange that served as a vacuum line from the cell and the second

welded flush with the side of the cell that served as the line to supply the test gas.

The axial hollow cathode glow discharge electrode assembly shown in Fig. 1 comprised a stainless steel plate (4.2 cm diameter, 0.9 mm thick) anode and a circumferential stainless steel cylindrical frame (5.1 cm OD, 7.2 cm long) perforated with evenly spaced 1 cm diameter holes. The cathode was attached to the cell body by a stainless steel wire covered with ceramic beads for electrical insulation, and the cell body was grounded.

A 1.6 mm thick UV-grade sapphire window with 1.5 cm view diameter provided a visible light path from inside the cell. The viewing direction was normal to the cell axis.

Strontium (Alfa Aesar 99.95%) metal was loaded into the cell under a dry argon atmosphere inside a glove box. The cell was evacuated with a turbo vacuum pump to a pressure of $\leqslant 0.0001$ Torr.

The gas in each experiment was ultrahigh purity grade or higher. Test gases comprised hydrogen, or krypton alone, helium–hydrogen mixture ($\frac{95}{5}$%), argon–hydrogen mixture ($\frac{95}{5}$%), or krypton–hydrogen mixture ($\frac{95}{5}$%). The gas pressure inside the cell was maintained at 2 Torr with a hydrogen flow rate of 30 sccm, a noble gas flow rate of 30 sccm, or a noble gas flow rate of 28 sccm and a hydrogen flow rate of 2 sccm. Each gas flow was controlled by a 0–20 sccm range mass flow controller (MKS 1179A21CS1BB) with a readout (MKS type 246). The cell pressure was monitored by a 0–10 Torr MKS Baratron absolute pressure gauge. In the absence of gas flow, the gas supply tube pressure was essentially the cell pressure. The partial pressure of the strontium metal was determined by its equilibrium vapor pressure at the operating temperature of the cell as given in Table 1.

The discharge was started and maintained by a DC electric field in the hollow cathode supplied by a constant voltage DC power supply (Xantrex XRF 600-2). The input power was calculated as the product of the constant voltage times the current. The voltage between the cathode and anode was monitored by a digital multimeter (Digital Instruments 9300GB). A duplicate multimeter in series with the discharge gap was used to indicate the current. The power was increased by ramping the constant voltage.

2.3. Power balance measurements

The temperature response of the cell to input power for the test and control gases and metals was determined. The temperature at the two thermocouples was recorded and averaged about one hour after the cell had reached a thermal steady state. The time to reach a steady state temperature with each increase in the input power to the glow discharge was typically 3–4 h. At this point the power P_T lost from the cell was equal to the power supplied to the cell P_{in} plus any excess power P_{ex}.

$$P_T = P_{in} + P_{ex}. \tag{15}$$

Table 1
Vapor pressure of strontium metal versus temperature

T (°C)	Sr P_v (Torr)[a]
20	8.39E-21
70	1.27E-16
120	1.62E-13
170	4.05E-11
220	3.26E-09
270	1.16E-07
320	2.23E-06
370	2.69E-05
420	2.25E-04
470	1.41E-03
500	3.76E-03
520	6.95E-03
535	1.08E-02
540	1.24E-02
560	2.16E-02
600	6.06E-02
620	9.78E-02
650	1.93E-01

[a]Calculated [39].

Since the heat transfer was dominated by conduction from the outer cell walls, the temperature rise of the cell above ambient ΔT was modeled by a linear curve

$$\Delta T = aP_T + C \tag{16}$$

where a and C are constants for the least square curve fit of the cell temperature response to power input for the control experiments ($P_{ex} = 0$). ΔT was recorded as a function of input power P_{in} for noncatalyst krypton alone and krypton–hydrogen mixtures over the input power range of 35–165 W. The higher temperature produced by the catalyst gases compared with the control gases was representative of the excess power since the cell temperature rise was found to be insensitive to heat transfer mechanisms occurring inside of the cell — the transfer to the cell walls being very fast and heat loss from the wall to the outside ambient environment dominating the cell temperature. In the case of each catalyst run, the total output power P_T was determined by solving Eq. (16) using the measured ΔT. The excess power P_{ex} was determined from Eq. (15).

3. Results

3.1. Line broadening measurements

The results of the 656.2 nm Balmer α line width measured with a high resolution (±0.025 nm) visible spectrometer on glow discharge plasmas of a mixture of 10% hydrogen and 90% xenon, strontium with hydrogen, a mixture of 10% hydrogen and 90% helium, or argon, 10% hydrogen with

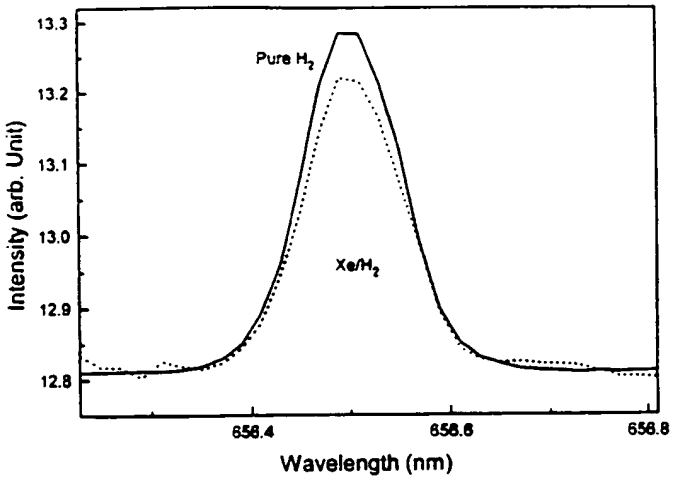

Fig. 3. The 656.2 nm Balmer α line width recorded with a high resolution (±0.025 nm) visible spectrometer on a xenon–hydrogen ($\frac{90}{10}$%) and a hydrogen glow discharge plasma. No line excessive broadening was observed corresponding to an average hydrogen atom temperature of ≈ 3 eV.

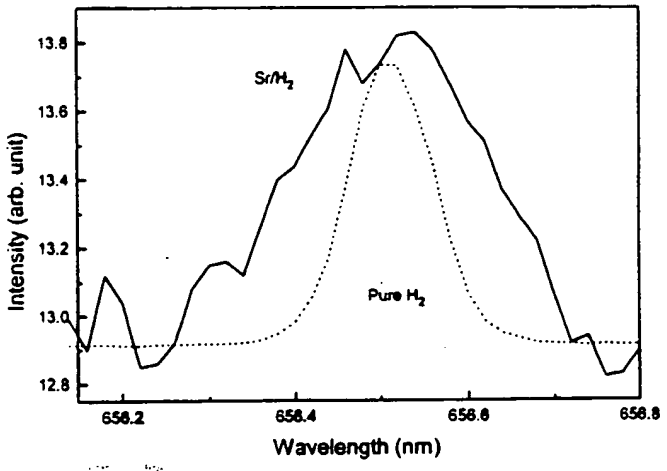

Fig. 4. The 656.2 nm Balmer α line width recorded with a high resolution (±0.025 nm) visible spectrometer on a strontium–hydrogen and a hydrogen glow discharge plasma. Significant broadening was observed corresponding to an average hydrogen atom temperature of 23–25 eV.

helium or argon and strontium each compared to control hydrogen alone are given in Figs. 3–8, respectively. To illustrate the method of displaying each line broadening result as an unsmoothed curve, the corresponding raw data points are also shown in Fig. 8 that further shows the scatter in the data. The Balmer α line width and energetic hydrogen atom densities and energies are given in Table 2. It was found that strontium–hydrogen, helium–hydrogen, argon–hydrogen, strontium–helium–hydrogen, and strontium–argon–hydrogen plasmas showed significant broadening corresponding to an average hydrogen atom temperature of 25–45 eV; whereas, pure hydrogen, krypton–hydrogen, xenon–hydrogen, and magnesium–hydrogen showed no excessive broadening corresponding to an average hydrogen atom temperature of ≈ 3 eV.

3.2. Power balance measurements

The temperature increase above the ambient temperature of 25 ± 0.1 °C as a function of the power applied to each of the gases and metal-gas mixtures at 2 Torr total pressure was plotted for the input power range of 35–160 W as shown

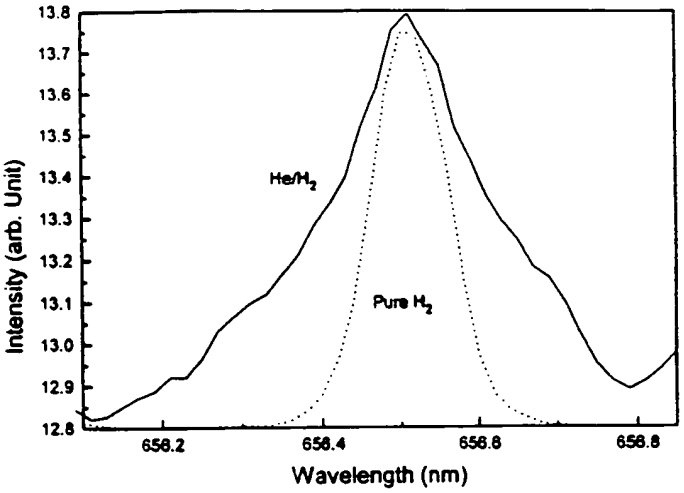

Fig. 5. The 656.2 nm Balmer α line width recorded with a high resolution (±0.025 nm) visible spectrometer on a helium–hydrogen ($\frac{90}{10}$%) and a hydrogen glow discharge plasma. Significant broadening was observed corresponding to an average hydrogen atom temperature of 30 -35 eV.

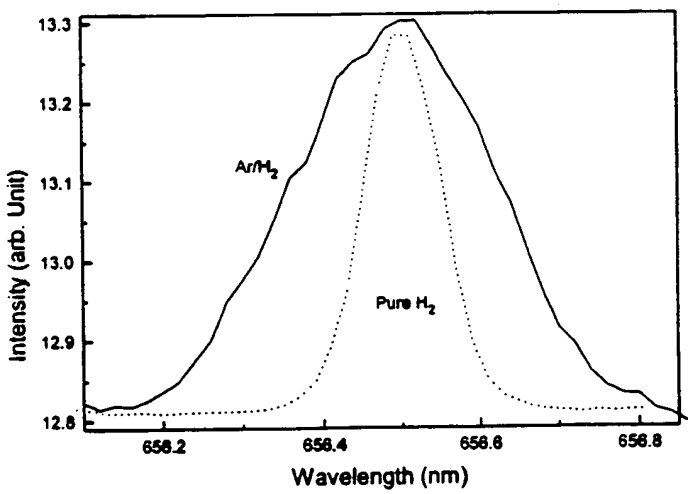

Fig. 6. The 656.2 nm Balmer α line width recorded with a high resolution (±0.025 nm) visible spectrometer on an argon–hydrogen ($\frac{90}{10}$%) and a hydrogen glow discharge plasma. Significant broadening was observed corresponding to an average hydrogen atom temperature of 30 -35 eV.

in Fig. 9. The least squares fit of the ΔT response to unit input power calculated from the control plasmas, krypton and krypton–hydrogen, (Eq. (16)) was determined to be

$$\Delta T = 7.25 + 0.687 \times P_T \quad (17)$$

where ΔT is in °C and P_T is in watts. At selected input powers, the total output power and excess power were determined using Eqs. (17) and (15), respectively, for (1) a mixture of hydrogen and vaporized strontium, (2) argon–hydrogen mixture ($\frac{95}{5}$%), and (3) a helium–hydrogen mixture ($\frac{95}{5}$%) or an argon–hydrogen mixture ($\frac{95}{5}$%) with vaporized strontium as shown Tables 3–6, respectively.

For a power input to the glow discharge of 110 W, the excess output power of mixtures of strontium with argon–hydrogen ($\frac{95}{5}$%), strontium with hydrogen, strontium with helium–hydrogen ($\frac{95}{5}$%), and argon–hydrogen ($\frac{95}{5}$%) was

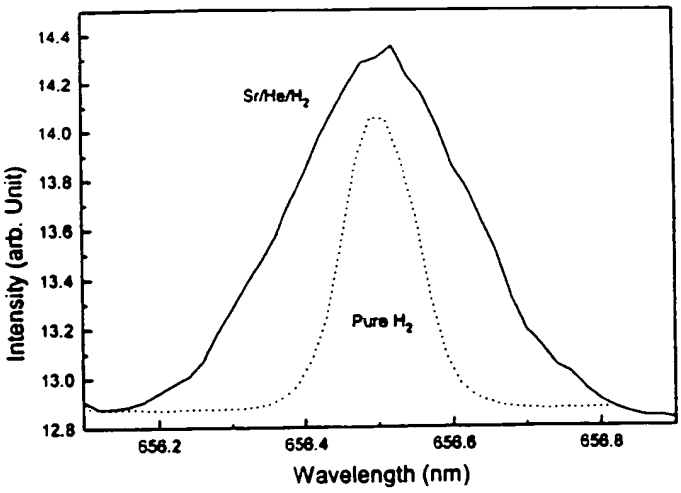

Fig. 7. The 656.2 nm Balmer α line width recorded with a high resolution (±0.025 nm) visible spectrometer on a strontium with helium–hydrogen ($\frac{90}{10}$%) and a hydrogen glow discharge plasma. Significant broadening was observed corresponding to an average hydrogen atom temperature of 40–45 eV.

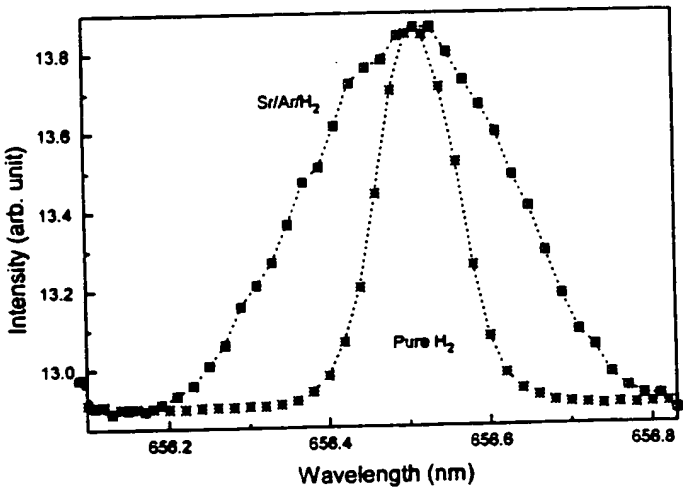

Fig. 8. The 656.2 nm Balmer α line width recorded with a high resolution (±0.025 nm) visible spectrometer on a strontium with argon–hydrogen ($\frac{90}{10}$%) and a hydrogen glow discharge plasma. Significant broadening was observed corresponding to an average hydrogen atom temperature of 35–40 eV.

75, 58, 50, and 28 W, respectively, based on a comparison of the temperature rise of the cell with krypton–hydrogen mixture ($\frac{95}{5}$%) and krypton alone. The input power was varied to determine conditions that resulted in the optimal output for the strontium–hydrogen plasma. As shown in Fig. 9 and Table 3, at 136 W input, the excess power significantly increased to 184 W. The effect was found to be repeatable in separate experiments.

4. Discussion

The Balmer α line width and energetic hydrogen atom density and energies were measured, and it was found that plasmas of strontium–hydrogen, argon–hydrogen, helium–hydrogen, and strontium with helium–hydrogen or argon–hydrogen showed significant broadening. Since line broadening is a measure of the plasma temperature, and

Table 2
The 656.5 nm Balmer α line width (full width at half maximum) and energetic hydrogen atom densities and energies for catalyst and noncatalyst plasmas

Plasma gas	Balmer α line FWHM (nm)	Hydrogen atom density[a] (10^{12} atoms/cm^3)	Hydrogen atom energy[b] (eV)
H_2	0.14	50	3–4
Mg/H_2	0.15	60	4–5
Kr/H_2	0.13	10	2.5–3.5
Xe/H_2	0.14	10	3–4
Sr/H_2	0.28	100	23–25
He/H_2	0.31	30	33–38
Ar/H_2	0.30	30	30–35
$Sr/He/H_2$	0.35	40	40–45
$Sr/Ar/H_2$	0.32	40	35–40

[a]Approximate calculated [38].
[b]Calculated [38].

a significant increase was observed with the presence of a catalyst, the power balances of glow discharge plasmas were measured.

Power production was observed from discharge plasmas having a source of hydrogen and atoms or ions which ionize at integer multiples of the potential energy of atomic hydrogen (Sr, He^+, or Ar^+); whereas, no excess power was observed in the case of krypton which does not provide a reaction with a net enthalpy of a multiple of the potential energy of atomic hydrogen under these conditions. Thermal power production was measured and observed from mixtures of strontium with argon–hydrogen ($\frac{95}{5}$%), strontium with hydrogen, strontium with helium–hydrogen ($\frac{95}{5}$%), and argon–hydrogen ($\frac{95}{5}$%). No possible chemical reactions of the 2 Torr or less hydrogen at a flow rate of 2 sccm, the electrodes, low pressure strontium, or the helium or argon gas could be found which accounted for the excess power of up to 184 W. In fact, no known chemical reaction releases enough energy (over 100 eV/H atom) to account for the power. The power was not observed when krypton or krypton–hydrogen replaced the argon–hydrogen or helium–hydrogen mixture. The power was commensurate with hydrogen fuel consumption. These results indicate that the power was due to a reaction of catalyst with hydrogen. The results of the power balance measurements are consistent with the line broadening measurements.

5. Conclusion

An average hydrogen atom temperature of 25–45 eV was observed by line broadening with the presence of strontium atoms or argon or helium ion catalysts; whereas, pure hydrogen, krypton–hydrogen, xenon–hydrogen, and magnesium–hydrogen plasmas showed no excessive broadening corresponding to an average hydrogen atom temperature of $\approx$ 3 eV. Excess thermal power was observed only with a catalyst present which demonstrated that line broadening was an effective method of measuring the catalysis reaction of hydrogen.

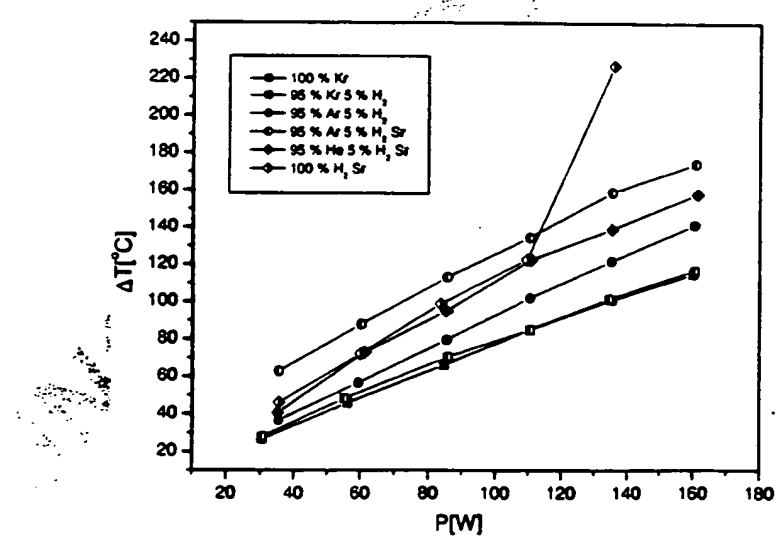

Fig. 9. The temperature increase above the ambient temperature of 25 ± 0.1°C as a function of the power applied to each of the gases and metal–gas mixtures. Significant excess power was observed in the case of catalyst–hydrogen plasmas (strontium, helium, and argon with hydrogen); whereas, no excess power was observed from noncatalyst–hydrogen plasmas.

Table 3
The total output power and excess power at selected input powers for the strontium–hydrogen plasma

Voltage (V)	Current (A)	Input power (W)	Temp. rise above ambient ΔT (±0.05°C)	Total output power P_T (±2%)	Excess power P_{ex} (±2%)
274	0.130	35.62	46.20	56.7	21.1
272	0.221	60.11	72.15	94.5	34.4
265	0.316	83.74	98.90	133.4	49.7
252	0.435	109.62	122.60	168.0	58.4
201	0.677	136.08	226.95	319.9	183.8

Table 4
The total output power and excess power at selected input powers for the argon–hydrogen plasma

Voltage (V)	Current (A)	Input power (W)	Temp. rise above ambient ΔT (±0.05°C)	Total output power P_T (±2%)	Excess power P_{ex} (±2%)
207	0.171	35.40	36.70	42.9	7.5
215	0.276	59.34	56.60	71.9	12.6
211	0.405	85.45	79.70	105.5	20.1
225	0.491	110.48	102.05	138.0	27.5
230	0.588	135.24	121.70	166.6	31.4
233	0.688	160.30	141.40	195.3	35.0

Table 5
The total output power and excess power at selected input powers for the strontium–helium–hydrogen plasma

Voltage (V)	Current (A)	Input power (W)	Temp. rise above ambient ΔT (±0.05°C)	Total output power P_T (±2%)	Excess power P_{ex} (±2%)
175	0.201	35.18	40.55	48.5	13.3
172	0.356	61.23	72.90	95.6	34.4
178	0.478	85.08	95.00	127.8	42.7
176	0.630	110.88	122.50	167.8	56.9
181	0.747	135.21	139.00	191.8	56.6
182	0.886	161.25	158.20	219.8	58.6

Table 6
The total output power and excess power at selected input powers for the strontium–argon–hydrogen plasma

Voltage (V)	Current (A)	Input power (W)	Temp. rise above ambient ΔT (±0.05°C)	Total output power P_T (±2%)	Excess power P_{ex} (±2%)
124	0.286	35.46	62.85	81.0	45.5
151	0.399	60.25	87.85	117.4	57.1
158	0.542	85.64	113.05	154.1	68.5
163	0.677	110.35	134.50	185.3	75.0
165	0.821	135.47	158.90	220.8	85.3
167	0.962	160.65	174.35	243.3	82.7

Excess power of up to 184 W by the catalytic reaction of strontium atoms, argon ions, or helium ions with atomic hydrogen corresponded to a volumetric power density of greater than 1 W/cm^3. This is comparable to many coal fired electric power plants. The presently observed and previously reported energy balances were over 100 eV/H atom [12,13]. The results are consistent with additional previously reported studies given in Section 1.2 which show very large energy balances.

Since the net enthalpy released may be over several hundred times that of combustion, the catalysis of atomic hydrogen represents a new source of energy with H_2O as the source of hydrogen fuel. Moreover, rather than air pollutants or radioactive waste, novel hydride compounds with poten-

tial commercial applications are the products [19–25]. Since the power is in the form of a plasma, direct high-efficiency, low cost energy conversion may be possible, thus, avoiding a heat engine such as a turbine [26,27] or a reformer-fuel cell system. Significantly lower capital costs and lower commercial operating costs than that of any known competing energy source are anticipated.

Acknowledgements

Special thanks to O. Klueva of Jobin Yvon Horiba, Inc, Edison, NJ for assistance and use of the high resolution spectrometer, and to Pamela McDonough for performing calorimetric experiments.

References

[1] Mills R. The grand unified theory of classical quantum mechanics. January 2000 Edition, Cranbury, New Jersey: BlackLight Power, Inc. Distributed by Amazon.com; posted at www.blacklightpower.com.

[2] Mills R. The grand unified theory of classical quantum mechanics. Global Foundation, Inc. Orbis Scientiae entitled The Role of Attractive and Repulsive Gravitational Forces in Cosmic Acceleration of Particles. The Origin of the Cosmic Gamma Ray Bursts, (29th Conference on High Energy Physics and Cosmology Since 1964) Dr. Behram N. Kursunoglu, Chairman, December 14–17, 2000, Lago Mar Resort, Fort Lauderdale, FL, New York: Kluwer Academic/Plenum Publishers, 2000. p. 243–58.

[3] Mills R. The grand unified theory of classical quantum mechanics. Int J Hydrogen Energy, in press.

[4] Mills R. The hydrogen atom revisited. Int J Hydrogen Energy 2000;25(12):1171–83.

[5] Mills R. The nature of free electrons in superfluid helium — a test of quantum mechanics and a basis to review its foundations and make a comparison to classical theory. Int J Hydrogen Energy 2001;26(10):1059–96.

[6] Mills R, Ray P. Spectral emission of fractional quantum energy levels of atomic hydrogen from a helium–hydrogen plasma and the implications for dark matter. Int J Hydrogen Energy, in press.

[7] Mills R, Ray P. Vibrational spectral emission of fractional-principal-quantum-energy-level hydrogen molecular ion. Int J Hydrogen Energy, in press.

[8] Mills R, Ray P. Spectroscopic identification of a novel catalytic reaction of potassium and atomic hydrogen and the hydride ion product. Int J Hydrogen Energy, in press.

[9] Mills R. Spectroscopic identification of a novel catalytic reaction of atomic hydrogen and the hydride ion product. Int J Hydrogen Energy 2001;26(10):1041–58.

[10] Mills R, Nansteel M. Argon–hydrogen–strontium plasma light source. IEEE Trans Plasma Sci, submitted.

[11] Mills R, Nansteel M, Lu Y. Excessively bright hydrogen–strontium plasma light source due to energy resonance of strontium with hydrogen. Eur J Phys D, submitted.

[12] Mills RL, Ray P, Dhandapani B, Nansteel M, Chen X, He J. New power source from fractional quantum energy levels of atomic hydrogen that surpasses internal combustion. Spectrochimica Acta, in progress.

[13] Mills R, Greenig N, Hicks S. Optically measured power balances of anomalous discharges of mixtures of argon, hydrogen, and potassium, rubidium, cesium, or strontium vapor. Int J Hydrogen Energy, submitted.

[14] Mills R, Nansteel M, Lu Y. Observation of extreme ultraviolet hydrogen emission from incandescently heated hydrogen gas with strontium that produced an anomalous optically measured power balance. Int J Hydrogen Energy 2001;26(4):309–26.

[15] Mills R, Dong J, Lu Y. Observation of extreme ultraviolet hydrogen emission from incandescently heated hydrogen gas with certain catalysts. Int J Hydrogen Energy 2000;25:919–43.

[16] Mills R. Observation of extreme ultraviolet emission from hydrogen–KI plasmas produced by a hollow cathode discharge. Int J Hydrogen Energy 2001;26(6):579–92.

[17] Mills R. Temporal behavior of light-emission in the visible spectral range from a Ti-K_2CO_3-H-Cell. Int J Hydrogen Energy 2001;26(4):327–32.

[18] Mills R, Onuma T, Lu Y. Formation of a hydrogen plasma from an incandescently heated hydrogen-catalyst gas mixture with an anomalous afterglow duration. Int J Hydrogen Energy 2001;26(7):749–62.

[19] Mills R, Dhandapani B, Nansteel M, He J, Voigt A. Identification of compounds containing novel hydride ions by nuclear magnetic resonance spectroscopy. Int J Hydrogen Energy 2001;26(9):965–79.

[20] Mills R, Dhandapani B, Greenig N, He J. Synthesis and characterization of potassium iodo hydride. Int J Hydrogen Energy 2000;25(12):1185–203.

[21] Mills R. Novel inorganic hydride. Int J Hydrogen Energy 2000;25:669–83.

[22] Mills R. Novel hydrogen compounds from a potassium carbonate electrolytic cell. Fusion Technol 2000;37(2):157–82.

[23] Mills R, Dhandapani B, Nansteel M, He J, Shannon T, Echezuria A. Synthesis and characterization of novel hydride compounds. Int J Hydrogen Energy 2001;26(4):339–67.

[24] Mills R. Highly stable novel inorganic hydrides. J Mater Res, submitted.

[25] Mills R, Good W, Voigt A, Jinquan Dong. Minimum heat of formation of potassium iodo hydride. Int J Hydrogen Energy 2001;26(11):1199–208.

[26] Mills R. Blacklight power technology — a new clean hydrogen energy source with the potential for direct conversion to electricity. Proceedings of the national hydrogen association, 12th Annual US Hydrogen Meeting and Exposition, Hydrogen: The Common Thread, The Washington Hilton and Towers, Washington DC, March 6–8, 2001. p. 671–97.

[27] Mills R. Blacklight power technology — a new clean energy source with the potential for direct conversion to electricity. Global Foundation International Conference on "Global Warming and Energy Policy", Dr. Behram N. Kursunoglu, Chairman, Fort Lauderdale, FL, New York: Kluwer Academic/Plenum Publishers, November 26–28, 2000. p. 1059–96.

[28] Sidgwick NV. The chemical elements and their compounds, vol. I. Oxford: Clarendon Press, 1950. p. 17.

[29] Lamb MD. Luminescence spectroscopy. London: Academic Press, 1978. p. 68.

[30] Linde DR. CRC handbook of chemistry and physics. 79th Edition, Boca Raton, Florida: CRC Press, 1998–9. p. 10–175 to p. 10–177.
[31] Boumans PWJM. Spectrochim. Acta B 1991;46:711.
[32] Broekaert JAC. Appl Spectrosc 1995;49:12A.
[33] Boumans PWJM, Broekaert JAC, Marcus, RK, editors. Spectrochim. Acta Part B, 1991;46:457.
[34] Dogan M, Laqua K, Massmann H. Spektrochemische Analysen mit einer Glimmentladungslampe als Lichtquelle — I. Spectrochim Acta B 1971;26:631–49.
[35] Dogan M, Laqua K, Massmann H. Spektrochemische Analysen mit einer Glimmentladungslampe als Lichtquelle — II. Spectrochim Acta B 1972;27:65–88.
[36] Broekaert JAC. J. Anal. Atmos. Spectrom. 1987;2:537.
[37] Kuraica M, Konjevic N. Line shapes of atomic hydrogen in a plane-cathode abnormal glow discharge. Phys Rev A 1992;46(7):4429–32.
[38] Videnocic IR, Konjevic N, Kuraica MM. Spectroscopic investigations of a cathode fall region of the Grimm-type glow discharge. Spectrochimica Acta B 1996;51:1707–31.
[39] Linde DR. CRC Handbook of Chemistry and Physics. 76th Edition, Boca Raton, FL: CRC Press, 1996. p. 4–121.